Research Article

Dynamic Reliability Prediction of Bridges Based on Decoupled SHM Extreme Stress Data and Improved BDLM

Xueping Fan [ID] **and Yuefei Liu**

Key Laboratory of Mechanics on Disaster and Environment in Western China (Lanzhou University),
The Ministry of Education of China, School of Civil Engineering and Mechanics, Lanzhou University, Lanzhou 730000, China

Correspondence should be addressed to Xueping Fan; fanxp@lzu.edu.cn

Bridge health monitoring system has produced a huge amount of monitored data (extreme stress data, etc.) in the long-term service periods; how to reasonably predict structural dynamic reliability with these data is one key problem in structural health monitoring (SHM) field. In this paper, considering the coupling, randomness, and time variation of SHM data, firstly, the coupled extreme stress data, which are considered as a time series, are decoupled into high-frequency and low-frequency data with the moving average method. Secondly, Bayesian dynamic linear models (BDLM) without priori monitoring error data (e.g., unknown monitored error variance) are built to dynamically predict the decoupled extreme stress; furthermore, the dynamic reliability of bridge members is predicted with the built BDLM and first-order second moment (FOSM) reliability method. Finally, an actual example is provided to illustrate the feasibility and application of the proposed models and methods. The research results of this paper will provide the theoretical foundations for structural reliability prediction.

1. Introduction

Bridge health monitoring systems have produced a huge amount of monitored data in the long-term service periods. How to reasonably predict and evaluate the dynamic reliability of bridge structures with these data is still at the initial stage at home and abroad. Nowadays, some achievements have been made. For example, Ni et al. [1] firstly proposed the concept of bridge reliability assessment based on structural health monitoring (SHM) data; Frangopol et al. [2] firstly provided the engineering application example of bridge reliability assessment based on SHM data; in the same year, the reliability evaluation and prediction methods of bridge dynamic performance based on SHM extreme stress data were also given [3, 4]; Liu et al. [5] directly evaluated the structural reliability based on the live load effects of the bridge health monitoring system; Li [6] analyzed and solved the reliability indices of bridge structures based on the SHM data; Jiao et al. [7] studied the performance assessment method of bridge structures through combining the SHM

data with the reliability method; Zhao [8] analyzed the reliability of Changchun Yitong bridge based on the ARMA model and the SHM data; Wang [9] proposed a new combinatorial method of vehicle and temperature load effects, which provided a reasonable information processing method for bridge reliability assessment; Fan [10] predicted the dynamic reliability indices of I-39 North Bridge and Yitong River Bridge based on SHM data and the Bayesian dynamic models; Fan et al. [11] carried out dynamic linear modeling of SHM data and structural reliability analysis; Wang et al. [12] forecasted temperature-induced strain of the long-span bridge with an improved Bayesian dynamic linear model. However, in the reliability analysis processes, the coupled characteristics of SHM data are not taken into account, which affects reliability analysis accuracy. Therefore, considering the coupled characteristics of SHM data, how to establish the dynamic prediction models of decoupled load effects with the SHM coupled load effects and dynamically predict bridge reliability should be further studied.

In this paper, taking into account the randomness and coupling of SHM data, the SHM data was decoupled into high-frequency and low-frequency data for eliminating the coupling factors of load effects (Section 2). Based on the distribution characteristics of decoupled health monitoring data, Bayesian dynamic linear models without priori monitoring error data (unknown monitored error variance) are built to predict the structural decoupled extreme stress (Section 3). Finally, the dynamic reliability analysis of the bridge member is carried out through combining SHM data with the reliability method (Sections 4 and 5).

2. Decoupling of SHM Data

The moving average methods used for decoupling of SHM data usually include the single moving average method, moving weighted average method, and trend moving average method. In this paper, with the widely used single moving average method, the low-frequency information in the coupled monitoring data is extracted, and the approximate high-frequency information is obtained through using the coupling information minus the low-frequency information. The detailed descriptions about the single moving average method are described as follows.

Suppose that there is time-series data: $y_1, y_2, \ldots, y_t, \ldots$; according to the single moving average method, the average value of N sequent time-series points can be obtained:

$$
\begin{aligned}
F_t^{(1)} &= \frac{y_t + y_{(t-1)} + \cdots + y_{t-N+1}}{N} \\
&= F_{(t-1)}^{(1)} + \frac{y_t - y_{(t-N)}}{N}, \quad t \geq N,
\end{aligned}
\tag{1}
$$

where $F_t^{(1)}$ is the moving average of the period, y_t is the monitoring data at time t, and N is the number of moving average number of items.

The single moving average method can eliminate certain interference factors of the SHM data and also easily predict the value of the next cycle, and the prediction formula is

$$
\widehat{y}_{(t+1)} = F_t^{(1)}.
\tag{2}
$$

3. Bayesian Dynamic Linear Models and Their Probability Recursive

In general, the prior monitored error information of Bayesian dynamic linear models (BDLM) is difficult to obtain. Therefore, this paper constructs the improved BDLM without the priori monitored error information (unknown monitored error variances). This model firstly determines the initial information of state θ_t and the prior distribution of monitored error v_t and state error ω_t. Set that monitored precision $\phi = V^{-1}$, v_t follows normal distribution $N(0, V)$, where V is the unknown constant variance. ω_t follows the T distribution $T(0, W_t)$.

3.1. Bayesian Dynamic Linear Models (BDLM). In this paper, BDLM of two random variables, which, respectively, represent high-frequency load effect and low-frequency load

effect, are built, and the probability parameters of decoupling load effect are recursively analyzed.

Monitored equation:

$$
\begin{aligned}
y_{i,t} &= \theta_{i,t} + v_{i,t}, \\
v_{i,t} &\sim N_i(0, V_i), \\
i &= 1, 2.
\end{aligned}
\tag{3}
$$

State equation:

$$
\begin{aligned}
\theta_{i,t} &= \theta_{i,(t-1)} + \omega_{i,t}, \\
\omega_{i,t} &\sim T_{i,n_{(t-1)}}(0, W_{i,t}), \\
i &= 1, 2.
\end{aligned}
\tag{4}
$$

Initial state information:

$$
\left(\theta_{i,(t-1)} | D_{i,(t-1)}\right) \sim T\left(m_{i,(t-1)}, C_{i,(t-1)}\right), \quad i = 1, 2,
\tag{5}
$$

$$
\left(\phi_i | D_{i,(t-1)}\right) \sim \Gamma\left(\frac{n_{i,(t-1)}}{2}, \frac{d_{i,(t-1)}}{2}\right), \quad i = 1, 2,
\tag{6}
$$

where $i = 1$ represents the low-frequency load effect, $i = 2$ represents the high-frequency load effect, $y_{i,t}$ is the monitored data at time t, $v_{i,t}$ is the monitored error which usually follows normal distribution, $\omega_{i,t}$ is the state error which usually follows T distribution, V_i and $W_{i,t}$ are, respectively, the variances of the monitored error and state error, $\mathbf{D}_{i,t}$ is the information set at and before time t, $m_{i,t}$ is the mean value of the state variable at time t, and $C_{i,t}$ is the variance of the state variable at time t. Suppose that $v_{i,t}$ and $\omega_{i,t}$ are internally independent, mutually independent, and independent of $\theta_{i,t}$ and $y_{i,t}$. Let $C_{i,t}$ and $m_{i,t}$ be approximately statistically obtained with the information set $\mathbf{D}_{i,t}$.

3.2. Probability Recursion of BDLM

(1) The posteriori distribution of state variable $\theta_{i,(t-1)}$, $i = 1, 2$, at time $(t-1)$: for mean $m_{i,(t-1)}$ and variance $C_{i,(t-1)}$, there are

$$
\begin{aligned}
\left(\theta_{i,(t-1)} | \mathbf{D}_{i,(t-1)}\right) &\sim T\left(m_{i,(t-1)}, C_{i,(t-1)}\right), \\
\left(\phi_i | \mathbf{D}_{i,(t-1)}\right) &\sim \Gamma\left(\frac{n_{i,(t-1)}}{2}, \frac{d_{i,(t-1)}}{2}\right).
\end{aligned}
\tag{7}
$$

(2) The priori distribution of state variable $\theta_{i,t}$, $i = 1, 2$ at time t:

$$
\left(\theta_{i,t} | \mathbf{D}_{i,(t-1)}\right) \sim T\left(a_{i,t}, R_{i,t}\right),
\tag{8}
$$

where $a_{i,t} = m_{i,(t-1)}$, $R_{i,t} = C_{i,(t-1)} + W_{i,t}$.

(3) One-step prediction distribution of monitored variable $y_{i,t}$, $i = 1, 2$ at time t:

$$
\left(y_{i,t} | \mathbf{D}_{i,(t-1)}\right) \sim T\left(\mu_{i,t}, Q_{i,t}\right),
\tag{9}
$$

where $\mu_{i,t} = a_{i,t}$, $Q_{i,t} = R_{i,t} + S_{i,(t-1)}$, and $P_t = \left(Q_{i,t}\right)^{-1}$ is the prediction precision of BDLM.

(4) The posteriori distribution of state variable $\theta_{i,t}$, $i = 1, 2$ at time t:

$$\left(\theta_{i,t}|\mathbf{D}_{i,t}\right) \sim T\left(m_{i,t}, C_{i,t}\right),$$
$$\left(\phi_i|\mathbf{D}_{i,t}\right) \sim \Gamma\left(\frac{n_{i,t}}{2}, \frac{d_{i,t}}{2}\right), \qquad (10)$$

where $C_{i,t} = (S_{i,t}/S_{i,(t-1)}) \times [R_{i,t} - A_{i,t}^2 Q_{i,t}]$, $m_{i,t} = a_{i,t} + A_{i,t} e_{i,t}$, $A_{i,t} = R_{i,t}(Q_{i,t})^{-1}$, $A_{i,t}$ is adaptive coefficient, and $e_{i,t} = y_{i,t} - f_{i,t}$ (one-step prediction error):

$$f_{i,t} = \mu_{i,t},$$
$$n_{i,t} = n_{i,(t-1)} + 1,$$
$$d_{i,t} = d_{i,(t-1)} + \frac{S_{i,t-1}e_{i,t}^2}{Q_{i,t}}, \qquad (11)$$
$$S_{i,t} = \frac{d_{i,t}}{n_{i,t}}.$$

According to the definition of the highest posterior density (HPD) region [10, 11], the prediction interval for the kth monitored data with a 95% confidential interval at time t is

$$\left[f_{i,t}(k) - 1.645\sqrt{Q_{i,t}(k)}, f_{i,t}(k) + 1.645\sqrt{Q_{i,t}(k)}\right]. \qquad (12)$$

3.3. Main Probability Parameters of BDLM.

The main probability distribution parameters about BDLM include $S_{i,(t-1)}$, $W_{i,t}$, $m_{i,(t-1)}$, $C_{i,(t-1)}$, $n_{i,(t-1)}$, and $d_{i,(t-1)}$.

The parameter $S_{i,(t-1)} = (n_{i,(t-1)}/d_{i,(t-1)})$ is a priori point estimate of $V = \phi^{-1}$ which can be approximately statistically obtained with the monitored data. The prior mean of ϕ at time t is $E[\phi_i|D_{i,(t-1)}] = (n_{i,(t-1)}/d_{i,(t-1)}) = (1/S_{i,(t-1)})$. The variance $W_{i,t}$ of the state error can be approximately determined with

$$W_{i,t} = -C_{i,(t-1)} + \frac{C_{i,(t-1)}}{\delta_i}, \qquad (13)$$

where δ_i is the discount factor, $\delta_1 = \delta_2 = 0.98$.

$m_{i,(t-1)}$ and $C_{i,(t-1)}$ can be estimated with the initial state information of the random variable at time t. In order to further study the influence of the parameter n_0 of the Γ distribution on the prediction precision of the BDLM proposed in the paper, the different values of the parameters n_0 are analyzed and studied.

4. Reliability Prediction of Bridge Structures

4.1. First-Order Second Moment (FOSM) Method.

Assume that the resistance R and the load effect S are independent of each other. The FOSM method is used to calculate the reliability indices. The mean and standard deviation of R and S are, respectively, μ_R, σ_R and μ_S, σ_S.

The supposed limit state function is

$$g(R, S) = R - S. \qquad (14)$$

FOSM-based reliability indices calculation equation is

$$\beta = \frac{\mu_R - \mu_S}{\sqrt{\sigma_R^2 + \sigma_S^2}}. \qquad (15)$$

4.2. Reliability Indices' Calculation of Bridge Structures.

In this paper, the adopted limit state function of bridge structures [3, 4, 10, 11] is

$$g(R, S, C, M) = R - S - C - \gamma_P(M_T + M_V), \qquad (16)$$

where R is the yield strength of steel, S is the stress of steel, C is the stress of concrete, M_T is the temperature load effect, M_V is the vehicle load effect, and γ_P is the sensor correction factor.

With equation (15), reliability indices prediction equation can be obtained with

$$\beta_P = \frac{\mu_R - \mu_S - \mu_C - \gamma_P\left(\mu_{M_T} + \mu_{M_V}\right)}{\sqrt{\sigma_R^2 + \sigma_S^2 + \sigma_C^2 + \left(\gamma_P\sigma_{M_T}\right)^2 + \left(\gamma_P\sigma_{M_V}\right)^2}}, \qquad (17)$$

where $(\mu_{M_T}, \sigma_{M_T})$ are the one-step predicted mean and standard deviation of BDLM about the temperature load effect, $(\mu_{M_V}, \sigma_{M_V})$ are the one-step predicted mean and standard deviation of BDLM about the vehicle load effect, (μ_R, σ_R) is, according to the design specification, the mean and standard deviation of the resistance, (μ_S, σ_S) is the mean and standard deviation of the stress of steel, (μ_C, σ_C) is the mean and standard deviation of the stress of concrete, and γ_P is the sensor correction factor.

5. Application to an Existing Bridge

In this paper, a five-span combined continuous steel plate girder bridge (I-39 Northbound Bridge) [3, 4, 10, 11] is taken as an actual example. The bridge was built in 1961 with a total length of 188.81 meters.

5.1. Extreme Stress Data Decoupling.

In this paper, the extreme stress about the midspan position of the transverse second-span in the I-39 Northbound bridge is monitored for 83 days. The monitoring data mainly include the temperature load effect data and the vehicle load effect data. This 83-day SHM stress data ensures that the correct distribution characteristics about the high-frequency and low-frequency data can be, respectively, and reasonably extracted. The monitored extreme stress data of 83 days is shown in Table 1. The 83-day extreme stress time-history curve is shown in Figure 1.

From Figure 1, it can be seen that the monitored stress is generally fluctuating at 25 MPa. The single moving average method is used to extract the trend items (low-frequency load effects) of monitored coupled extreme stress data. The difference between the primary time curve and the trend curve is taken as the bridge stress caused by the vehicle loads,

Table 1: Monitored extreme stress data for 83 days.

t	σ	t	σ	t	σ	t	σ	t	σ	t	σ	t	σ
1	25.23	13	20.6	25	30.51	37	22.83	49	23.01	61	24.61	73	32.92
2	21.67	14	22.56	26	21.57	38	21.05	50	22.02	62	22.11	74	21.94
3	19.53	15	23.54	27	31.67	39	24.44	51	33.9	63	21.22	75	21.14
4	20.5	16	16.94	28	29.16	40	28.8	52	18.1	64	25.15	76	20.41
5	24.44	17	29.16	29	21.67	41	20.24	53	25.24	65	24.64	77	16.76
6	22.66	18	22.47	30	23.99	42	29.97	54	25.77	66	23.18	78	22.38
7	25.95	19	23.37	31	21.05	43	24.17	55	17.11	67	21.94	79	27.21
8	32.65	20	28.99	32	29.35	44	23.72	56	23.72	68	18.82	80	19.98
9	39.26	21	30.15	33	22.66	45	26.85	57	12.65	69	22.66	81	18.82
10	21.4	22	21.22	34	24.61	46	30.32	58	24.89	70	21.57	82	29.44
11	31.48	23	22.02	35	25.77	47	31.93	59	27.56	71	29.16	83	20.41
12	30.06	24	34.8	36	28.54	48	25.06	60	25.86	72	21.57		

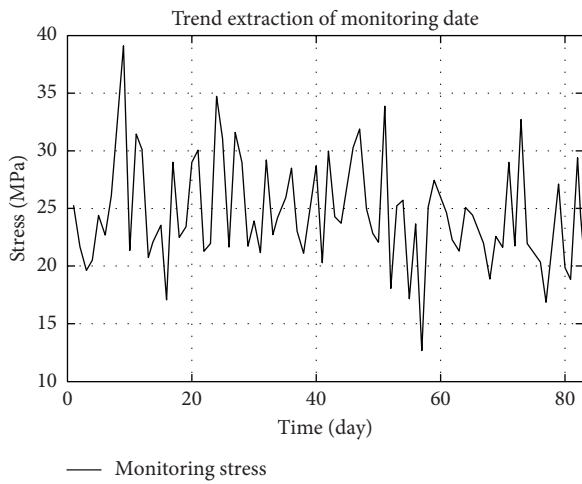Note: t is the time, days; σ is the stress, MPa.
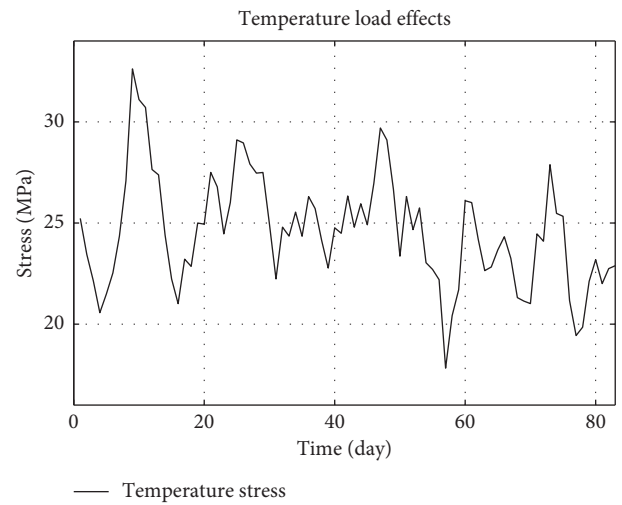

Figure 1: Monitored stress for 83 days.

Figure 2: Decoupled temperature load effects for 83 days.

namely, the high-frequency load effects; furthermore, the decoupling between the vehicle load effect and the temperature load effect is realized.

In this paper, the single moving average method is adopted to carry out extreme stress decoupling. The fluctuation of other random load effects (not including the temperature load effect and the vehicle load effect) is thought to be negligible, and the time curves and data of the temperature load effect are obtained with the single moving average method shown in Figure 2 and Table 2.

The difference between the initial time curves and the trend curves is taken as the bridge extreme stress caused by the vehicle loads. The vehicle load effect and the temperature load effect are decoupled. The results are shown in Figure 3 and Table 3.

5.2. Kendall Rank Correlation Test.
The Kendall rank correlation test was performed on the decoupling stress data with SPSS statistical software. The test results are shown in Table 4.

From Table 4, the Kendall rank correlation coefficient of two random variables is 0.016, and the significance (two-tailed) probability is 0.835. Therefore, it is assumed that the decoupling stress signals (high-frequency load effects and low-frequency load effects) are independent of each other.

5.3. BDLM of Decoupling Extreme Stress Data.
The monitoring extreme stress data are decoupled with the single moving average method, and 83 days decoupling temperature load effect data and vehicle load effect data are obtained, as shown in Table 2 and Table 3.

The following is to determine the main probability parameters for building BDLM. $\phi = V^{-1}$, $v_{i,t}$ follows normal distribution $N(0, V_i)$, V_i is the unknown constant variance, and $\omega_{i,t}$ follows T distribution $T_i(0, W_{i,t})$. In this paper, the monitored extreme stress data are decoupled into two random variables which are approximately as the respective initial state data. The initial state information is estimated and the mean and variance of the initial information are obtained with equation (20).

With equations (3)–(6), BDLM with unknown observational variances can be obtained with the following equations.

TABLE 2: Decoupling temperature load effects' data for 83 days.

t	σ	t	σ	t	σ	t	σ	t	σ	t	σ	t	σ
1	25.23	13	27.38	25	29.11	37	25.71	49	26.67	61	26.01	73	27.88
2	23.45	14	24.41	26	28.96	38	24.14	50	23.36	62	24.19	74	25.48
3	22.14	15	22.23	27	27.92	39	22.77	51	26.31	63	22.65	75	25.33
4	20.57	16	21.01	28	27.47	40	24.76	52	24.67	64	22.83	76	21.16
5	21.49	17	23.21	29	27.50	41	24.49	53	25.75	65	23.67	77	19.44
6	22.53	18	22.86	30	24.94	42	26.34	54	23.04	66	24.32	78	19.85
7	24.35	19	25.00	31	22.24	43	24.79	55	22.71	67	23.25	79	22.12
8	27.09	20	24.94	32	24.80	44	25.95	56	22.20	68	21.31	80	23.19
9	32.62	21	27.50	33	24.35	45	24.91	57	17.83	69	21.14	81	22.00
10	31.10	22	26.79	34	25.54	46	26.96	58	20.42	70	21.02	82	22.75
11	30.71	23	24.46	35	24.35	47	29.70	59	21.70	71	24.46	83	27.88
12	27.65	24	26.01	36	26.31	48	29.10	60	26.10	72	24.10		

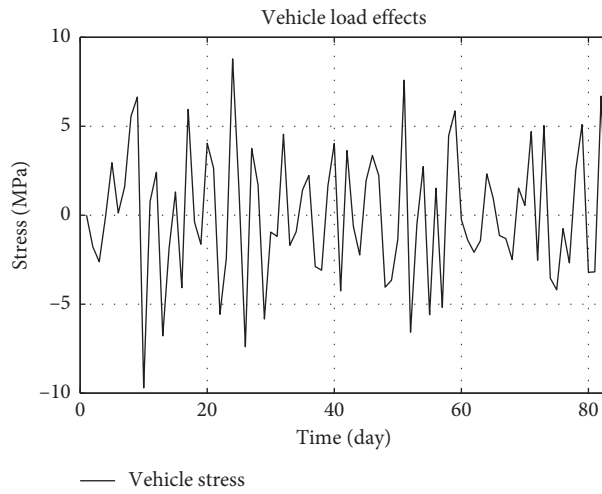Note: t is the time, days; σ is the stress, MPa.

FIGURE 3: Decoupled vehicle load effects for 83 days.

TABLE 3: Decoupling vehicle load effects' data for 83 days.

t	σ	t	σ	t	σ	t	σ	t	σ	t	σ	t	σ
1	0.00	13	−6.78	25	1.40	37	−2.88	49	−3.66	61	−1.40	73	5.04
2	−1.78	14	−1.85	26	−7.39	38	−3.09	50	−1.34	62	−2.08	74	−3.54
3	−2.61	15	1.31	27	3.75	39	1.67	51	7.59	63	−1.43	75	−4.19
4	−0.07	16	−4.07	28	1.69	40	4.04	52	−6.57	64	2.32	76	−0.75
5	2.95	17	5.95	29	−5.83	41	−4.25	53	−0.51	65	0.97	77	−2.68
6	0.13	18	−0.39	30	−0.95	42	3.63	54	2.73	66	−1.14	78	2.53
7	1.60	19	−1.63	31	−1.19	43	−0.62	55	−5.60	67	−1.31	79	5.09
8	5.56	20	4.05	32	4.55	44	−2.23	56	1.52	68	−2.49	80	−3.21
9	6.64	21	2.65	33	−1.69	45	1.94	57	−5.18	69	1.52	81	−3.18
10	−9.70	22	−5.57	34	−0.93	46	3.36	58	4.47	70	0.55	82	6.69
11	0.77	23	−2.44	35	1.42	47	2.23	59	5.86	71	4.70	83	−2.48
12	2.41	24	8.79	36	2.23	48	−4.04	60	−0.24	72	−2.53		

Note: t is the time, days; σ is the stress, MPa.

Monitored equation:

$$
\begin{aligned}
y_{i,t} &= \theta_{i,t} + v_{i,t}, \\
v_{i,t} &\sim N(0, V).
\end{aligned}
\tag{18}
$$

State equation:

$$
\begin{aligned}
\theta_{i,t} &= \theta_{i,(t-1)} + \omega_{i,t}, \\
\omega_{i,t} &\sim T_{i,n_{(t-1)}}(0, W_{i,t}).
\end{aligned}
\tag{19}
$$

TABLE 4: Kendall rank correlation test.

	Correlation test	Temperature load effects' data	Vehicle load effects' data
		Correlation coefficient	1.000	0.016
	Temperature load effects' data	Sig. (two-tailed)	0	0.835
		N	83	83
Kendall's tau_b		Correlation coefficient	0.016	1.000
	Vehicle load effects' data	Sig. (two-tailed)	0.835	0
		N	83	83

Initial state information:

$$\left(\theta_{i,(t-1)}|D_{i,(t-1)}\right) \sim \mathrm{T}\left(m_{i,(t-1)}, C_{i,(t-1)}\right), \tag{20}$$

$$\left(\phi_i|D_{i,(t-1)}\right) \sim \Gamma\left(\frac{n_{i,(t-1)}}{2}, \frac{d_{i,(t-1)}}{2}\right), \tag{21}$$

where $y_{i,t}$ is the monitoring extreme stress data of the temperature load effect ($i = 1$) and the vehicle load effects ($i = 2$) at time t. According to the authors' engineering experience, the initial parameter $n_{i,0}$ is adopted as 83. $d_{i,(t-1)}$ can be calculated by the priori point estimate $S_{i,(t-1)} = (n_{i,(t-1)}/d_{i,(t-1)})$ based on initial information; $\omega_{i,t}$ is the state error of the BDLM. $W_{i,t} = -C_{i,(t-1)} + (C_{i,(t-1)}/\delta_i)$, where $\delta_1 = \delta_2 = 0.98$; $C_{i,(t-1)}$ can be obtained the decoupled extreme stress data.

In the paper, BDLM with no prior information distribution (unknown monitored variances) is established to predict the extreme stress of 83 days. The predicted data of the temperature load effects are shown in Figure 4 and the prediction precision is shown in Figure 5. The predicted data of the vehicle load effects are shown in Figure 6 and the prediction precision is shown in Figure 7. From Figures 4 and 6, it can be seen that the prediction results can effectively explain the range and trend of decoupled dynamic monitoring data. Figures 6 and 7 show that the prediction precision increases with the distant updating of monitored data.

In order to further understand the effects of the Γ distribution parameter $n_{i,0}$ on the prediction precision, the initial parameters $n_{1,0}$ of the temperature load effect are analyzed with different values ($n_{1,0} = 20, 80$), as shown in Figure 8, which show that the prediction accuracy curve tends to be smooth with the increase of the parameter n_0 and be increasing in a certain interval.

5.4. Dynamic Reliability Prediction.

In this paper, the bridge is a five-span combined continuous steel plate girder bridge (I-39 Northbound Bridge) [3, 4, 10, 11]. The basic design information for the bridge is as follows:
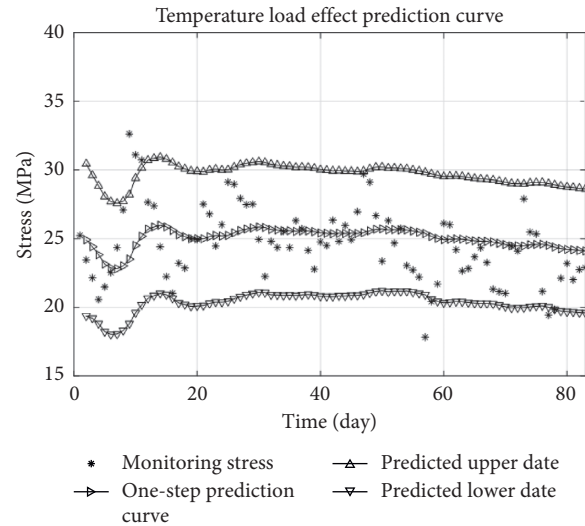

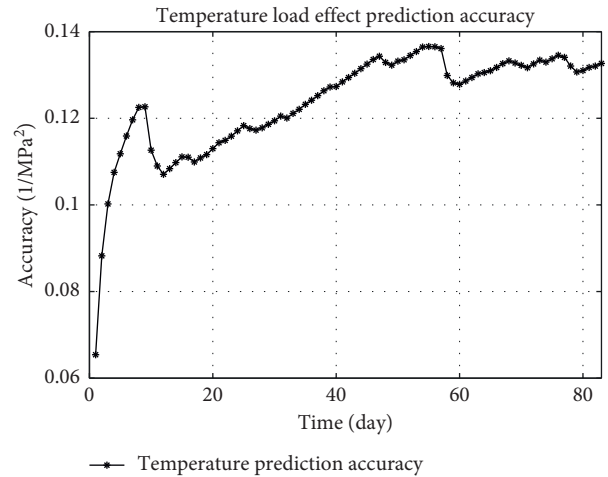FIGURE 4: Predicted temperature load effects.

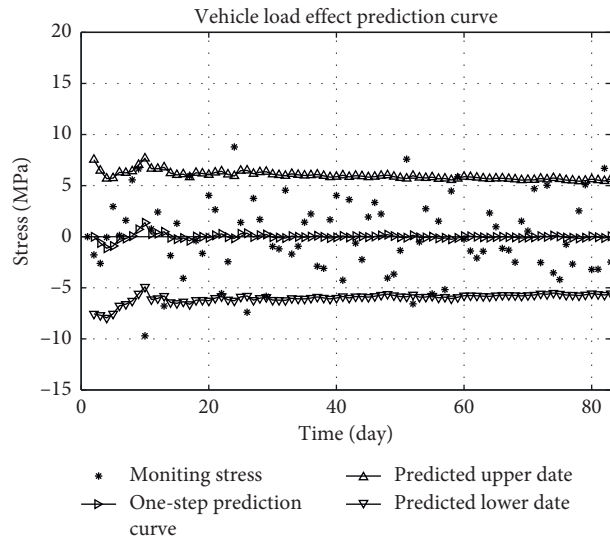FIGURE 5: Prediction precision of temperature load effects.
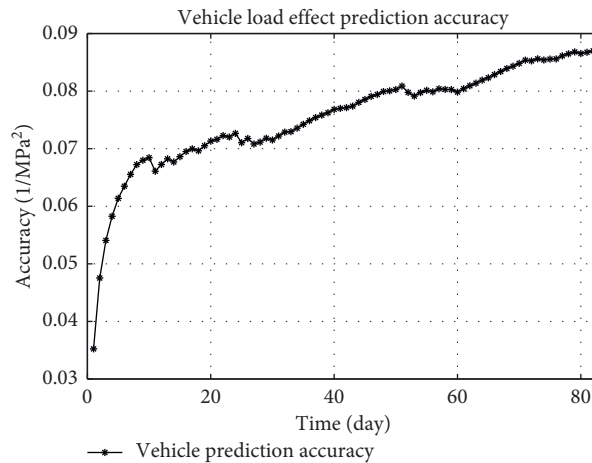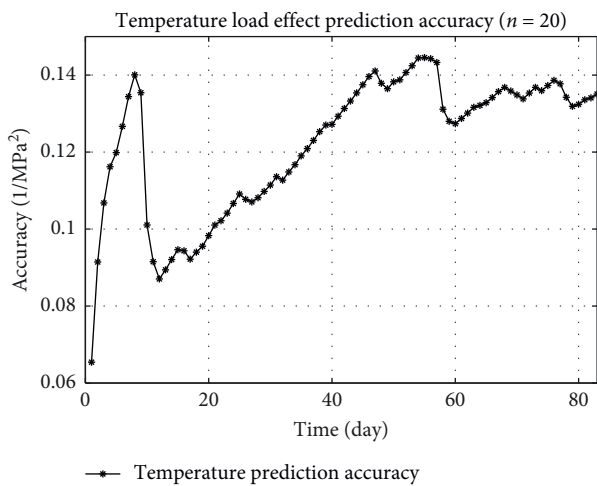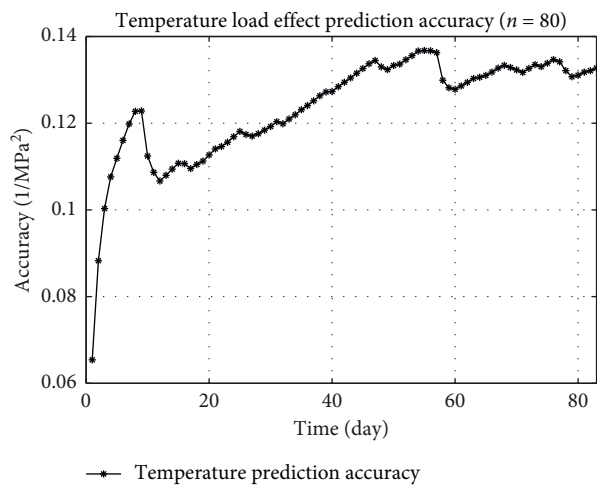
FIGURE 6: Predicted vehicle load effects.

FIGURE 7: Prediction precision of vehicle load effects.

FIGURE 8: The curve of prediction accuracy with the different parameter $n_{1,0}$. (a) $n_{1,0} = 20$. (b) $n_{1,0} = 80$.

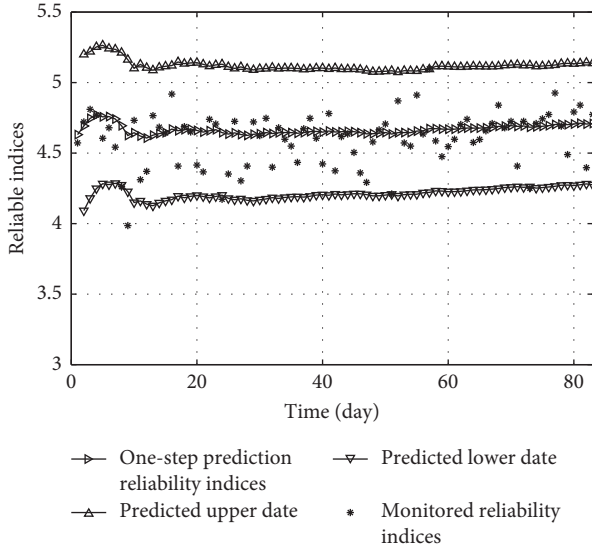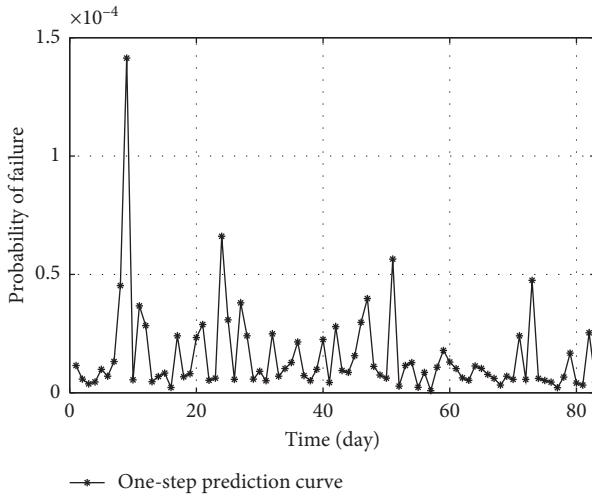Figure 9: Predicted bridge reliability indices.

Figure 10: Predicted bridge failure probability.

$$\mu_R = 380\text{MPa},$$
$$\sigma_R = 26.6\text{MPa},$$
$$\mu_S = 116.3\text{MPa},$$
$$\sigma_S = 4.65\text{MPa}, \qquad (22)$$
$$\mu_S = 108.8\text{MPa},$$
$$\sigma_S = 4.35\text{MPa},$$
$$\gamma_P = 1.15.$$

With equation (17), there is

$$\beta_P = \frac{155 - 1.15 \times \left(\mu_{M_T} + \mu_{M_V}\right)}{\sqrt{27.351^2 + \left(1.15 \times \sigma_{M_T}\right)^2 + \left(1.15 \times \sigma_{M_V}\right)^2}}, \qquad (23)$$

where $(\mu_{M_T}, \sigma_{M_T}^2)$ are the one-step forward predicted mean and variance of temperature load effects and $(\mu_{M_V}, \sigma_{M_V}^2)$ are the one-step forward predicted mean and variance of the vehicle load effects.

FOSM method is used to predict the dynamic reliability indices of bridge structure, and the reliability indices of the 83-day real-time monitoring data are compared and analyzed, as shown in Figure 9. The change trends of the real-time monitoring reliability indices can be explained well with that based on the BDLM proposed by this paper and the FOSM method.

The failure probability of the bridge member is calculated with equation (24). The results are shown in Figure 10:

$$p_f = \Phi(-\beta). \qquad (24)$$

Figure 10 shows that the failure probability of the bridge member in the I-39 North Bridge is less than 1.5×10^{-4}. Therefore, the bridge member is safe and reliable.

6. Conclusions

In this paper, the monitored coupled extreme stress data are decoupled into high-frequency and low-frequency extreme stress data for eliminating the influence of coupling factors. The Kendall rank correlation coefficient is introduced to analyze the correlation between the decoupled extreme stress data. BDLM is constructed to predict decoupling monitored extreme stress data. With the FOSM method, the reliability indices of the bridge member are predicted and analyzed.

The useful results are summarized as follows:

(1) The reliability indices of the bridge members are predicted by decoupling the coupled monitoring data, which effectively eliminates the influence of the coupling factors between the decoupled load effects.

(2) BDLM (unknown observational variances) can be used to predict and analyze the dynamic monitored extreme stress and the dynamic reliability indices of bridge members. The prediction results can effectively explain the range and trend of decoupled real-time monitoring data.

(3) The Γ-distribution parameter n_0 and the time parameter of BDLM are two factors that affect the variation curve of prediction precision. The prediction precision increases with time. The prediction accuracy curve tends to be smooth with the increase of the parameter n_0 and be increasing in a certain interval.

Data Availability

The data used to support the findings of the study are available from the corresponding author upon request.

Conflicts of Interest

The authors declare no conflicts of interest with respect to the research, authorship, and/or publication of this article.

Acknowledgments

References

[1] Y. Q. Ni, X. G. Hua, and J. M. Ko, "Reliability-based assessment of bridges using long-term monitoring data," *Key Engineering Materials*, vol. 321, pp. 217–222, 2006.

[2] D. M. Frangopol, A. Strauss, and S. Y. Kim, "Bridge reliability assessment based on monitoring," *Journal of Bridge Engineering, ASCE*, vol. 13, no. 3, pp. 258–270, 2008.

[3] D. M. Frangopol, A. Strauss, and S. Y. Kim, "Use of monitoring extreme data for the performance prediction of structures: general approach," *Engineering Structures*, vol. 30, pp. 3644–3653, 2008.

[4] A. Strauss, D. M. Frangopol, and S. Y. Kim, "Use of monitoring extreme data for the performance prediction of structures: Bayesian updating," *Engineering Structures*, vol. 30, pp. 3654–3666, 2008.

[5] M. Liu, D. M. Frangopol, and S. Y. Kim, "Bridge safety evaluation based on monitored live load effects," *Journal of Bridge Engineering*, vol. 14, no. 4, pp. 257–269, 2009.

[6] S. L. Li, *Approaches of Condition Assessment and Damage Alarming of Bridges Based on Structural Health monitoring*, Harbin Institute of Technology, Harbin, China, 2009.

[7] M. J. Jiao, L. M. Sun, and Q. F. Li, "Bridge structural reliability assessment based on health monitoring data," *Journal of Tongji University (Natural Science)*, vol. 39, no. 10, pp. 1452–1457, 2011.

[8] Z. Zhao, *Health Monitoring Data Modeling and Reliability Analysis for Yitong River Bridge Based on ARMA model*, Harbin Institute of Technology, Harbin, China, 2012.

[9] Z. J. Wang, *A New Combination Method of Vehicle and Temperature Load Effects Based on SHM data*, Harbin Institute of Technology, Harbin, China, 2012.

[10] X. P. Fan, *Reliability Updating and Bayesian Prediction of Bridges Based on Proof Loads and Monitored data*, Harbin Institute of Technology, Harbin, China, 2014.

[11] X. P. Fan, Y. F. Liu, and D. G. Lu, "Dynamic linear modeling of bridge monitored data and reliability prediction," *Journal of Tongji University (Natural Science)*, vol. 44, no. 7, pp. 1002–1009, 2016.

[12] H. Wang, Y. M. Zhang, J. X. Mao, H. P. Wan, T. Y. Tao, and Q. X. Zhu, "Modeling and forecasting of temperature-induced strain of a long-span bridge using an improved Bayesian dynamic linear model," *Engineering Structures*, vol. 192, pp. 220–232, 2019.